# A Single-Chip AlScN PMUTs-on-CMOS Hydrophone

Eyglis Ledesma, Arantxa Uranga, and Núria Barniol, *Member, IEEE*

***Abstract*—This work presents a minute single-chip piezoelectric micromachined ultrasonic transducers (PMUTs)-on-complementary metal-oxide-semiconductor (CMOS)-based hydrophone with high receiving sensitivities and low noise. The system is based on three different $Sc_{9.5\%}$ $Al_{90.5\%}$ N PMUTs geometries: (a) square with an 80 $\mu$m side, (b) rectangular with a dimension of 60 × 40 $\mu$m, and (c) annular with an outer diameter of 80 $\mu$m which allows to carry out acoustic measurements at very close distances from the transducer under test. Each device is monolithically integrated with a CMOS low noise amplifier (LNA) amplifier with a gain of 25 dB. The first hydrophone prototype was validated in water where two commercial hydrophones from ONDA (HGL-0085 and HNC-0200) were used as references. The experimental results give mean receiving sensitivities of −234 dB re 1 V/$\mu$Pa (equivalent to 1.9 V/MPa), −234.6 dB re 1 V/$\mu$Pa (equivalent to 1.86 V/MPa), and −238.3 dB re 1 V/$\mu$Pa (equivalent to 1.22 V/MPa) for (a)–(c), respectively. These results demonstrate the high performance of the presented PMUTs-on-CMOS to be used in a miniaturized hydrophone for characterizing high-frequency ultrasound transducers.**

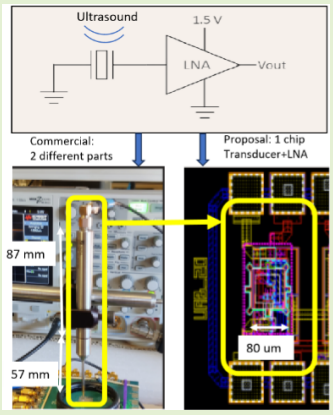


***Index Terms*—Hydrophone, micro-electro-mechanical-system (MEMS) hydrophone, piezoelectric micromachined ultrasonic transducers (PMUTs), PMUTs-on-complementary metal-oxide-semiconductor (CMOS), receiving sensitivity (SR).**

## I. Introduction

HYDROPHONES, in the ultrasonic field, can be described as devices designed to convert underwater acoustic pressure into electrical signals [1]. They allow us to characterize ultrasound transducers in terms of instantaneous acoustic pressure, acoustic intensity, peak compressional (P+) and peak rarefactional (P−) pressures, etc. For biomedical acoustic devices, these magnitudes are important to determine parameters such as the mechanical index (MI), which indicates some possible bioeffects (nonthermal), such as cavitation, by giving a measurement of the ultrasonic energy applied to a patient during an ultrasound examination [2]. Based on that, the use of hydrophones covers several biomedical fields in order to guarantee the safety of medical procedures, avoid harm to health, and provide figures to meet the specifications provided by standards and regulatory bodies [3]. For instance, the ultrasound probes used in applications such as diagnostic which include high-resolution images of organs and fetuses [4], neuromodulation [5], and therapeutic treatments including drug delivery [6], require a previous characterization with a hydrophone before going on the market. Recently hydrophones have been widely described in [3] for assessment of biomedical devices and in [7] focused on sonar devices for ranging applications requiring lower frequency operation.

Focusing on piezoelectric hydrophones for biomedical applications, they can be mainly classified as: 1) membrane; 2) needle; and 3) capsule. The first one consists of one or more thin films of piezoelectric polymer (e.g., PVDF) that are supported in a ring (large dimensions) keeping it tense and where only a small area is activated. These offer a flat response over a broad bandwidth, however, at low MHz frequencies the directional response is limited to 37°. On the other hand, needle hydrophones are based on a piezoelectric element (piezo-ceramic or piezo-polymer) placed on the tip of a central conductor. In this case, the frequency response is the least flat, affected by the resonance due to the thickness of the piezoelectric, scattering, and diffraction effects at the edge of the needle. Finally, capsule hydrophones offer a better form factor than membrane reducing some artifacts as

Manuscript received 19 March 2024; revised 9 May 2024; accepted 13 May 2024. Date of publication 23 May 2024; date of current version 1 July 2024. This work was supported in part by the Spanish Ministry of Science and Innovation under Project PID2019-108270RB-I00 and Project PID-2022-136624OB-100. The associate editor coordinating the review of this article and approving it for publication was Prof. Jean-Michel Redoute. *(Corresponding author: Arantxa Uranga.)*

The authors are with the Department of Electronics Engineering, Universitat Autònoma de Barcelona, 08193 Barcelona, Spain (e-mail: Eyglis.Ledesma@uab.cat; Arantxa.Uranga@uab.cat; Núria.Barniol@uab.cat).

Digital Object Identifier 10.1109/JSEN.2024.3401455

a consequence of the diffraction effect, and their frequency response is flatter than needle. Unlike membrane hydrophones, capsule and needle hydrophones are suitable for placing closer to the emitting transducer due to their reduced form factor [1], [3]. Onda Corporation [8] and Precision Acoustics [9] are two of the most important companies dedicated to fabricating and commercializing hydrophones. Their catalog shows models where the piezoelectric element can reach very small dimensions such as 85 $\mu$m (Capsule hydrophone HGL-0085 from ONDA) with a nominal sensitivity of $-278$ dB (re 1 V/$\mu$Pa and without any amplifier) and 40 $\mu$m (Needle hydrophone NH0040 from Precision Acoustics) with a nominal sensitivity of $-284.4$ dB (re 1 V/$\mu$Pa with an external preamplifier).

The importance of developing hydrophones suitable for high-performance biomedical applications regardless of the size of the transmitting transducer, its frequency, and the working distance has become a challenge today. Some researchers and companies are addressing this challenge, for instance, a patent published in 2023 by FUJIFILM Sonosite Inc. Ivanytskyy et al. [10] proposes a membrane hydrophone with an active area between 10 and 30 $\mu$m suitable for high-frequency applications. Another approach of a membrane hydrophone was proposed in 2016, where a 30 $\mu$m active area was calibrated to 110 MHz with a mean sensitivity of 30 nV/Pa [11]. However, like any membrane-based hydrophones, the large encapsulation size makes them not proper to calibrate small ultrasound systems, for example, in intravascular ultrasound systems (IVUS) catheters with dimensions lower than 1.5 mm [12]. In this context, the fast growth of the micro-electro-mechanical-system (MEMS) industry has allowed the development and study of the potentialities of small new hydrophone systems based on micromachined ultrasonic transducers (MUTs). This technology provides a robust fabrication process allowing small sizes, large sensitivities, and the capability to integrate the transducers with the complementary metal-oxide-semiconductor (CMOS) circuitry. MUTs can be classified according to their working principle in capacitive MUTs (CMUTs) and piezoelectric MUTs (PMUTs).

A hydrophone based on a 2-D CMUT array was validated in [13]. This system proposes 256 elements (arranged in 16 $\times$ 16 CMUTs), giving a total dimension of 4 $\times$ 4 mm and where an application-specific integrated circuit (ASIC) was flip-chip bonded. The sensitivity at the amplifier output ranges from 1 to 76 $\mu$V/Pa using dc vias from 0.95 to 30.85 V with operation frequencies below 2 MHz. Unlike CMUTs, PMUTs do not require polarization voltages to ensure their correct behavior during reception which provides low power consumption and less complex connections. PMUTs in receive mode are based on the direct piezoelectric effect where an incoming ultrasound wave causes a deflection of the membrane which produces mechanical stress on the piezoelectric layer and is detected by measuring the voltage signal between the top and bottom electrodes surrounding the piezoelectric layer. This is another benefit compared to CMUTs because receiving sensitivity (SR) is not related to cavity height.

PMUTs-based hydrophones have been reported in the state-of-the-art [14], [15], [16]. In [14], a 3.2 $\times$ 3.2 mm$^2$ AlN PMUT array and its preamplifier chip are connected in a printed circuit board and packaged in a final hydrophone holder with dimensions of 1.5 $\times$ 0.8 $\times$ 2 cm. The SR of this system offers a flat response with a considerable SR of $-178 \pm 0.5$ dB (re: 1 V/$\mu$Pa) over the low-frequency range between 10 Hz to 50 kHz and a frequency range not suitable for the assessment of biomedical devices acoustic performance. On the other hand, in [15], a 6 $\times$ 6 AlN PMUT array was presented even with slightly better sensitivity and SR of $-172.6$ dB (re: 1 V/$\mu$Pa) in the low-frequency range from 100 Hz to 2 kHz. As a final example of hydrophones based on PMUTs, a 9.5% Scandium-doped AlN array was discussed in [16]. In this case, the system uses the same structure proposed in [14], improving the SR to $-164.5 \pm 0.5$ dB (re: 1 V/$\mu$Pa) and also with the same low-frequency range as in [14]. From the presented results in these works, there are some aspects to highlight. The first one is related to the low operating frequency range, which despite the high sensitivity values achieved, is not suitable to characterize medical ultrasound devices (operating in MHz frequencies, for instance, the frequency of lithotripsy ranges from 0.2 to 0.9 MHz [17], for IVUS the operation frequency is in the range of 10's MHz [18]). The second aspect considers the conditioning circuitry where, like in all commercialized hydrophones, the needed preamplification is in a separated substrate (chip or package), requiring electrical connections between hydrophone and preamplifier, bigger overall sizes, affecting the performance of the received acoustic signals (degraded signal due to a large parasitic capacitance), and increasing the overall cost of the hydrophone system. Note that any commercial piezoelectric hydrophone requires a preamplifier (or adapting circuitry) to "make independent" the received signal by the hydrophone from the electrical load (which will depend on the cables used, the data acquisition system like oscilloscope, connectors, etc.). The hydrophone calibration is carried out against a fixed electrical load, and to guarantee this calibration, any user must use the same electrical charge. This is achieved by the preamplifier.

In this article, we overcome this last limitation, presenting a single-chip hydrophone based on a PMUT integrated monolithically with its CMOS preamplifier circuitry (PMUTs-on-CMOS) with great potential as a hydrophone system for biomedical devices assessment. The presented PMUTs-on-CMOS (with three different shapes: square, rectangular, and annular) offer small active areas (maximum side 80 $\mu$m) being suitable for measurements closer to the ultrasound transducer under test. The main contribution of this work is providing a single chip that includes the sensor element and the amplification, which reduces the total area and provides a cost-effective hydrophone system. The experimental results show that our PMUTs-on-CMOS-based hydrophones achieve a higher SR and lower noise compared to the commercial ones. After this introduction, Section II describes the main characteristics of the hydrophones; in Section III the design and fabrication of the PMUTs-on-CMOS are detailed; Section IV corresponds to the experimental results for our hydrophones and finally Section V provides a comparison of our PMUT-on-CMOS hydrophones with the commercial ones, demonstrating the

enhanced performance of the presented single-chip PMUT-on-CMOS hydrophones.

## II. Hydrophone Design Considerations

Hydrophone main characteristics depend on the applications for which they are intended, i.e., frequency range and maximum pressures. For instance, some diagnostic and therapeutic ultrasound devices can be found in a frequency range from 1 to 10 MHz with a maximum pressure of 1 MPa [17]. Once the application has been defined, there are several characteristic parameters that are important to consider when a hydrophone is designed, and they are listed as follows.

### A. Element Size and Spatial Averaging Effect

The hydrophone size is determined in order to avoid the spatial averaging effect [19], [20]. This phenomenon appears because the hydrophone does not measure the acoustic pressure at the center of its aperture, instead, it obtains the average acoustic pressure over the whole area of its sensing element. The effect causes an underestimation of the peak pressure and an overestimation of the beamwidth [7]. Some recommendations can be found in the literature that suggest hydrophone apertures compared with a half-wavelength [21] or a quarter-wavelength [11]. However, these approximations could be unreasonable in some scenarios where the wavelength is very small (e.g., a frequency of 60 MHz in water causes a wavelength of 25 $\mu$m being $\lambda/2 = 12.5$ $\mu$m and $\lambda/4 = 6.25$ $\mu$m). A more realistic method to determine the maximum hydrophone radius ($a_h$) is described in (1) where $\lambda$ is the wavelength, $a_t$ is the radius of the transducer under test, and $l$ is the distance between the hydrophone and the transducer [22]

$$a_h = \frac{\lambda}{8a_t}\left(\sqrt{l^2 + a_t^2}\right). \tag{1}$$

From this equation, the normalized distance of the hydrophone from the transducer ($l/2a_t$) can be obtained, as shown in Fig. 1 for different hydrophone radii. Considering the same ultrasound transducer ($2a_t$) and the same wavelength ($\lambda$) if the radius of the hydrophone increases, the minimum distance between it and the ultrasound transducer also increases. This means that small hydrophone dimensions are desired to measure acoustic pressures near the transducers under test. In addition, when the ultrasound transducer under test works at high frequencies (low wavelength), such as ultrasound devices for IVUS applications, small hydrophone apertures are required to measure the acoustic pressure close to the transducer surface.

### B. Directional Response

The directivity gives a measure of the variation in sensitivity when the angle between the acoustic signal and the active element of the hydrophone is changed. Equation (2) illustrates a general expression to compute it where $n$ can take values of 0, 1, or 2 for a piston, simply-supported or clamped transducer, respectively, $k$ is the wavenumber ($2\pi/\lambda$), $a_h$ is the radius of the hydrophone, $\theta$ is the incidence angle, and

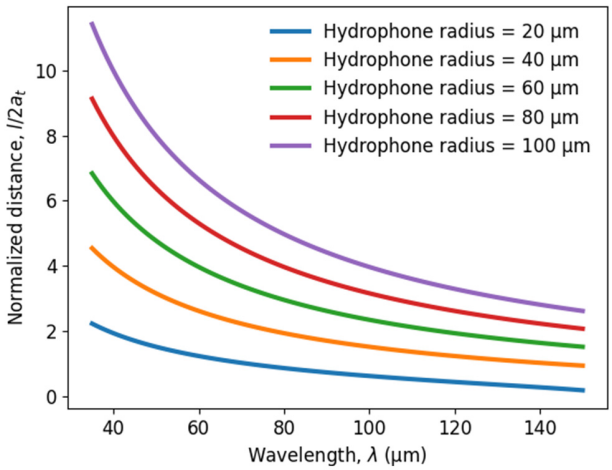


Fig. 1. Normalized distance of the hydrophone from the transducer ($l/2a_t$) dependence versus wavelength for different hydrophone radii.

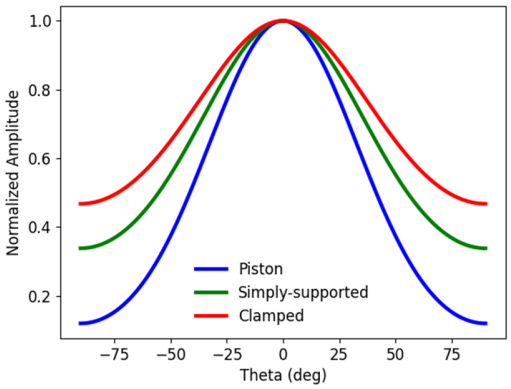


Fig. 2. Directivity computed for an 80 $\mu$m device at 20 MHz in water modifying the boundary conditions to: piston (blue solid line), simply-supported (green solid line), and clamped (red solid line).

$J_n()$ refers to Bessel function of order $n$ [23]

$$D(\theta) = \frac{2^{n+1}(n+1)!J_{n+1}(k{\cdot}a_h \cdot \sin(\theta))}{(k \cdot a_h \cdot \sin(\theta))^{n+1}}. \tag{2}$$

Based on (2), if $k \cdot a_h \ll 1$, it is possible to obtain an omnidirectional radiation pattern (the same sensitivity regardless of the incident angle); however, if $k \cdot a_h \gg 1$, the beam becomes more directional. As can be seen, the radius of the hydrophone plays an important role in the directivity because smaller apertures can allow for higher frequencies while maintaining the same sensitivity in all directions. Fig. 2 is obtained by plotting (2) considering an 80 $\mu$m device at 20 MHz in water and where the boundary conditions give a piston, a simple-supported, and a clamped device. From this graph, the clamped device offers a more omnidirectional pattern, ensuring a beamwidth at $-6$ dB higher than 150° instead of values close to 110° and 82° for simple-supported and piston devices, respectively.

### C. Sensitivity and Frequency Response

The sensitivity describes the capacity of the hydrophone to translate an acoustic pressure in a voltage signal and depends on the actuation frequency. An ideal hydrophone should have a

high sensitivity with a flat response in a broad frequency range. However, several factors affect it depending on the electrical setup. Equation (3) describes how the intrinsic or nominal sensitivity defined as "End-of-Cable Open Circuit Sensitivity" ($SR_{EOC}$) could be affected by some capacitances: SR is the loaded SR which depends on the measured values (*Acquired Voltage/Transmitted Pressure*) in the specific experimental set-up; $G$ is the amplifier gain; $C_H$ is the capacitance of the hydrophone; $C_A$ is the capacitance of the amplifier, and $C_P$ includes all parasitic capacitances due to cables, connectors, etc. [17]. Clearly, a decrease of the parasitic capacitances and the input capacitance of the amplifiers are desired to obtain higher receiving loaded sensitivity, SR. As we will show in Section III, this is the case for our PMUTs-on-CMOS integrated hydrophones

$$\mathrm{SR}\,(f) = G\,(f) \cdot \mathrm{SR_{EOC}}\,(f) \cdot \frac{C_H}{C_H + C_A + C_P}. \tag{3}$$

### D. Minimum and Maximum Pressure

The minimum measurable pressure is described by the noise equivalent pressure (NEP). For a correct acoustic pressure evaluation, the acoustic pressure value must be at least five or ten times higher than this factor [3], [17]. NEP can be computed using (4) where Noise corresponds to the electrical noise at the output of the amplifier and SR is the loaded SR of the hydrophone [1]

$$\mathrm{NEP\,[Pa]} = \frac{\mathrm{Noise}[\mu\mathrm{V}]}{\mathrm{SR}\left[\frac{\mathrm{nV}}{\mathrm{Pa}}\right]} * 1000. \tag{4}$$

On the other hand, the maximum pressure level is affected by: 1) the maximum pressure acquired by the hydrophone at which the amplifier is in its linear regime (given by the dynamic range of the amplifier) and 2) the signal level at which the hydrophone is not damaged due to, among other factors, some mechanical stress, or heating. Focus on 1) this value can be obtained using the $P_{-1\mathrm{dB}}$ compression point of the amplifier gain and will be the dominant factor for our integrated single-chip hydrophone.

## III. PMUT-on-CMOS Hydrophone: Design and Fabrication

The presented PMUTs-on-CMOS hydrophone is based on three different geometries (square, rectangular, and annular) of PMUTs integrated monolithically with the CMOS circuitry. The commercial MEMS-on-CMOS platform from Silterra, already validated for PMUTs devices [24], [25] was used to fabricate these prototypes. Specifically, the CMOS technology used is the Silterra CL130H32 1P6M (@1.5 V). Fig. 3(a) top shows a general block diagram of a single hydrophone based on PMUT-on-CMOS. The incoming ultrasound waves are transduced by the PMUT in which its top electrode is connected to the receiving channel (RX), while the bottom electrode is grounded. The RX block consists of a CMOS low noise amplifier (LNA) with a gain of 25 dB and a 50 Ω output buffer for testing purposes. The CMOS LNA is a voltage amplifier where the input voltage signal is generated from the integration of the PMUT's current on its input node.

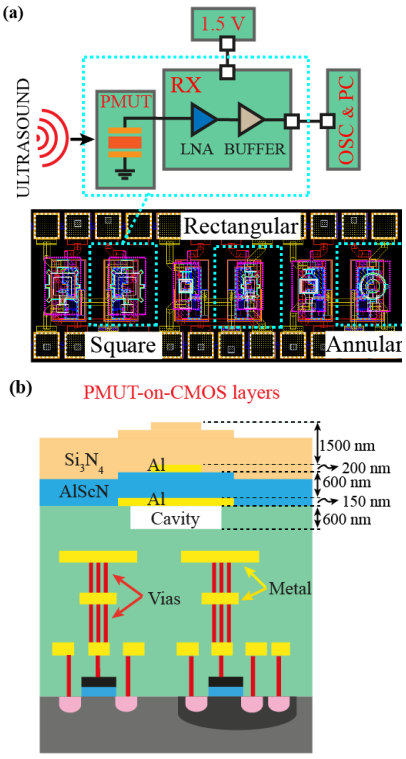


Fig. 3. (a) Block diagram of the proposed PMUT-on-CMOS hydrophone (top). Full layout of the system (PMUTs over the CMOS LNA front-end circuitry) where the used designs have been highlighted in cyan (bottom). (b) PMUT-on-CMOS schematic layer stack (thickness is not to scale).

To minimize power consumption, area, and noise, a self-biased CMOS inverter configuration is designed using a pMOS transistor operating in its sub-threshold region as a large feedback resistor (refer to [29] for a detailed description). The overall reception area is tiny ($6 \times 10^{-4}$ mm$^2$) which ensures a compact design where the total area will be limited, in our case, by the PMUTs dimensions.

Fig. 3(a) bottom shows the final layout of the PMUTs integrated over the CMOS LNA front-end along with the electrical pads. The used PMUTs as hydrophones have been highlighted in cyan. All PMUTs are clamped structures where some external holes outside the cavity were used to release the membrane with a height of 600 nm. These clamped PMUT structures are flexural resonators in their first out-of-plane mode.

Based on the shown layout (from left to right), the first device is a square membrane with a dimension of 80 $\mu$m, the second one is a rectangular structure with dimensions of 60 $\times$ 40 $\mu$m, and finally, the last one is an annular shape with outer and inner diameters of 80 and 40 $\mu$m, respectively. The dimensions were chosen to have PMUTs-on-CMOS systems with areas close or small to the commercial hydrophones provided by ONDA and then establish a fair comparison. Specifically, the areas of the three shaped PMUTs are: square PMUT (80 $\times$ 80 $\mu$m $=$ 6400 $\mu$m$^2$); rectangle PMUT (60 $\times$ 40 $\mu$m $=$ 2400 $\mu$m$^2$), and annular (3769 $\mu$m$^2$).

Fig. 3(b) illustrates a schematic cross section of a single PMUT-on-CMOS device. It consists of an unimorph layer of

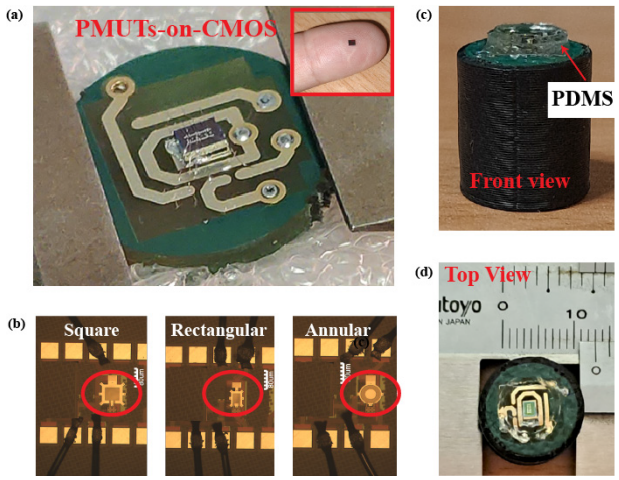


Fig. 4. Encapsulation structure for the first hydrophone prototype. (a) PMUTs-on-CMOS bonded to a dedicated PCB (1 cm diameter). Inset: chip over the author's finger. (b) Optical images of the square, rectangular, and annular PMUTs-on-CMOS used as hydrophones. (c) and (d) Front and top views of the final PMUTs-on-CMOS hydrophone covered with the PDMS.

600 nm of 9.5% Sc-doped AlN ($Sc_{9.5\%}Al_{90.5\%}N$) deposited by PECVD and sandwiched between two Al electrodes with thicknesses of 200 and 150 nm for top and bottom electrodes, respectively. The final PMUT layer is 1500 nm of $Si_3N_4$ which is used as an elastic layer providing insulation to the metal electrodes and waterproof capability. The interconnection between the PMUT electrodes and the CMOS metal layers was made using vias which reduces the parasitic capacitance compared to heterogeneous integration, such as flip-chip bonding [26] or eutectic wafer bonding [27]. Based on this, one of the benefits that monolithic integration provides is to improve the signal-to-noise ratio, likewise, the overall area is reduced compared to a commercial hydrophone and preamplifier system (larger than 100 mm) by providing, in the presented design, a single chip with a dimension of 1.9 × 1.5 mm with three read points and their respective LNAs. Note that the final configuration toward a commercial hydrophone based on this PMUT-on-CMOS technology could be only one of these PMUT layouts.

The first prototype (designed only for testing purposes) of the presented hydrophone based on PMUTs-on-CMOS devices consists of basically two elements: 1) a dedicated printing circuit board (PCB) and 2) a base structure. The PCB (∼1 cm in diameter) is designed as shown in Fig. 4(a) where the die is glued at the center and the electrical connections between the die and the PCB are made by dedicated wire bonding (25 $\mu$m Al wire). Connections to the power supply (1.5 V for biasing the CMOS LNA and ground) and oscilloscope (for reading the output LNA voltage) were done through a flexible cable placed in the back side of the PCB. Note that the dimensions of the chip are minute compared to the PCB, which will allow for a reduction in the future packaging of the hydrophone based on PMUTs-on-CMOS.

On the other hand, the base structure [shown in Fig. 4(c) and (d)] is a simple plastic cylinder that fixes the PCB and creates a structure to hold the system during the measurements. The final step consists of covering the system with a PDMS layer to provide protection for the bonding wires and ensure a high yield during the measurements in water. PDMS deposition is homemade, being challenging to guarantee uniformity in all directions by hand, however, an attempt was made to maintain 1.4 mm thickness in the active region. The optical images of the PMUTs-on-CMOS covered with PDMS are illustrated in Fig. 4(b).

TABLE I
ONDA'S HYDROPHONES AND PREAMPLIFIER CHARACTERISTICS

| Device | Parameters | Devices | |
|---|---|---|---|
| Hydrophone | Name | HGL-0085 | HNC-0200 |
| | Type | Capsule | Needle |
| | Diameter (µm) | 85 | 200 |
| | Nominal sensitivity (dB re: 1V/µPa) | -278 | -271 |
| | Nominal sensitivity (nV/Pa) | 13 | 28 |
| Pre-amplifier | Name | AG-2010 | AH-2010-025 |
| | Gain (dB) | 20 | 20 |
| | Noise@Bandwidth (µVrms@MHz) | 260@60 | 160@25 |

## IV. Results and Discussion

The acoustic characterization in water was carried out using a commercial ultrasound transducer from OPTEL as a transmitting element with a diameter of 5 mm and a central frequency of 5 MHz [28]. The pressure was measured using two commercial hydrophones from ONDA (connected to their respective preamplifiers) and our single-chip PMUTs-on-CMOS hydrophone. Table I summarizes the principal characteristics of the used ONDA's hydrophones and their preamplifiers.

The distance between the OPTEL and the hydrophone systems was determined according to (1) where the $a_t$ is 2.5 mm, $a_h$ varies according to Table I, and $\lambda$ corresponds to the minimum wavelength (maximum frequency) that is desired to measure. In order to reach frequencies in the water close to 20 MHz with the smallest commercial hydrophone (diameter of 85 $\mu$m), the distance between the OPTEL and this was fixed to 9 mm. However, due to its low sensitivity, echo amplitudes were too small for reliable measurement at higher frequencies, and therefore, the pressure could not be calibrated. For this reason, the HNC-0200 hydrophone was also used because its sensitivity is higher than the HGL-0085 hydrophone, although unfortunately at this distance, the uncertainty in the measurements increases above 10 MHz.

### A. Sensitivity and Frequency Response

To obtain the receiving loaded sensitivity (SR) of the presented PMUTs-on-CMOS hydrophones, the ultrasound transducer from OPTEL, was calibrated with the commercial hydrophones in water [see set-up Fig. 5(a)]. This step allows us to obtain the acoustic pressure at 9 mm in a frequency range from 1 to 10 MHz without spatial averaging artifacts using the HGL-0085. Once the pressure was obtained, each PMUT-based hydrophone was placed at the same axial

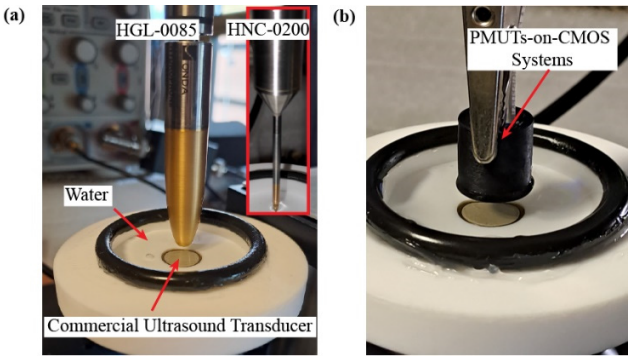


Fig. 5. Underwater experimental set-up: (a) using two commercial hydrophones from ONDA and (b) using the presented PMUTs-on-CMOS hydrophone.

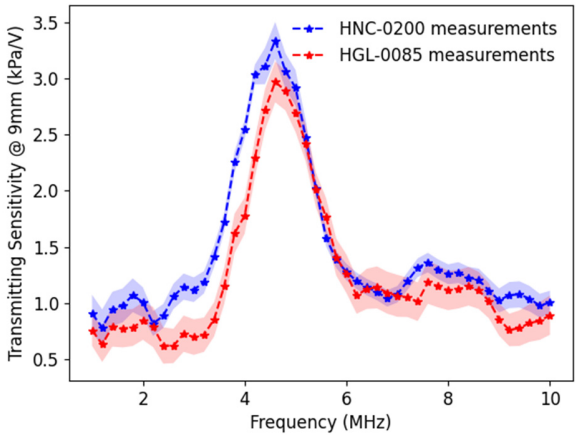


Fig. 6. Frequency response of the transmitting sensitivity at 9 mm using HNC-0200 (blue curve) and HGL-0085 (red curve) both for the OPTEL transducer.

position to ensure the same pressure level, and the voltage amplitudes at the CMOS-LNA output were acquired in the same frequency range. Considering these values, the SR was computed as the ratio between the voltage amplitudes and acoustic pressure at the same frequency.

To carry out this experiment, the OPTEL was driven with four sine-cycles with an amplitude of 23.8 $V_{pp}$ in a frequency range from 1 to 10 MHz with steps of 200 kHz and the HGL-0085 hydrophone was placed at 9 mm [see the set-up in Fig. 5(a)]. The measured pressure at each frequency was normalized with the applied voltage to the OPTEL transducer, and therefore, the dependence on the input voltage was avoided. The position in the plane ($x$–$y$-directions) was optimized using a manual micropositioner system when the ultrasound transducer was excited at 4.8 MHz (maximum echo amplitude) giving around 3 kPa/V at 9 mm from the transducer surface (see Fig. 6 red curve).

For comparison, the HNC-0200 hydrophone was also used in the same frequency range, see Fig. 6 blue curve. Note that there are some differences between both measurements, however, the behavior is the same, giving the peak frequency at 4.8 MHz. In the second step [see the set-up in Fig. 5(b)], the OPTEL was driven with four sine-cycles with 2.4 $V_{pp}$ at the same discrete frequencies, and the position in the plane for each PMUT was optimized. The SR was computed based on these values and the previously measured pressure. Fig. 7

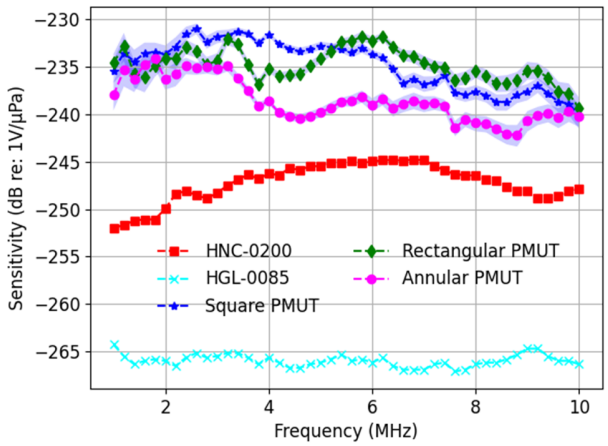


Fig. 7. Experimental receiving loaded sensitivity curve in water where: blue-stars, green diamonds, and magenta points correspond to the square, rectangular, and annular PMUTs-on-CMOS hydrophones. Red squares and cyan cross correspond to the commercial hydrophones from ONDA HNC-0200 and HGL-0085 with their respective preamplifiers which were extracted from the provided calibration given by the company.

illustrates the receiving sensitivities in dB re 1 V/$\mu$Pa for each single PMUT-on-CMOS and the commercial hydrophones for comparison. The uncertainty was estimated through the standard deviation ($\sigma_{SR}$), see (5), where $\sigma_{Amp}$ is the accuracy in measuring the amplitude, and $\sigma_{Pres}$ is the accuracy in measuring the acoustic pressure, giving a maximum error of 2 dB re 1 V/$\mu$Pa

$$\sigma_{SR} = \sqrt{\left(\frac{dSR}{dAmp} \cdot \sigma_{Amp}\right)^2 + \left(\frac{dSR}{dPres} \cdot \sigma_{Pres}\right)^2}. \quad (5)$$

From the results, the presented PMUTs-on-CMOS hydrophones achieve high receiving sensitivities with average values of −234 dB re 1 V/$\mu$Pa (equivalent to 1.9 V/MPa), −234.6 dB re 1 V/$\mu$Pa (equivalent to 1.86 V/MPa), and −238.3 dB re 1 V/$\mu$Pa (equivalent to 1.22 V/MPa) for square, rectangular, and annular PMUTs, respectively, over a bandwidth from 1 to 10 MHz. The sensitivities of commercial hydrophones were extracted from the given calibration from ONDA, and in both cases, the preamplifier gain was considered. Focusing on the square PMUT-on-CMOS hydrophone, the average SR is 30 dB higher than the HGL-0085 (with almost the same dimension) and 15 dB better than the HNC-0200 (with a dimension 60% small), demonstrating the potentialities of the presented PMUT-on-CMOS hydrophone.

Based on the loaded SR obtained, the nominal sensitivity for each PMUTs-on-CMOS was computed according to (3) where $G$ is the gain (25 dB), $C_H$ is the capacitance associated with physical layouts of PMUTs, $C_A$ is the LNA equivalent input capacitance considering the Miller effect [29], and $C_P$ is negligible for monolithic integrated systems. Substituting $C_{LNA}$ for 609 fF, and $C_{PMUT}$ for 496 fF if the PMUT is square, 186 fF if it's rectangular, or 584 fF if it's annular, the nominal sensitivity ($SR_{EOC}$) gives 238, 445, and 140 nV/Pa for the square, rectangular or annular PMUTs-on-CMOS-based hydrophones, respectively.

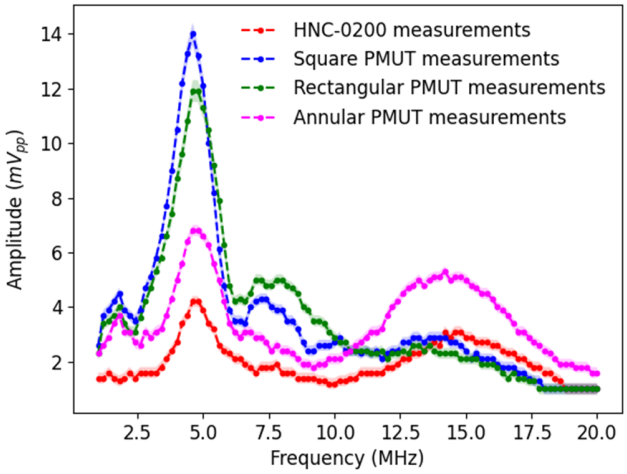


Fig. 8. Frequency response of the peak-to-peak amplitudes measured at 9 mm and applying 2.4 Vpp to the commercial ultrasound transducer with (a) HNC-0200 (red curve), (b) square PMUT-on-CMOS (blue curve), (c) rectangular PMUT-on-CMOS (green curve), and (d) annular PMUT-on-CMOS (magenta curve).

Comparing the 80 $\mu$m square PMUT-on-CMOS with the HGL-0085, an improvement of an 18.3× factor is achieved, which could be increased to 34 times with a smaller area if the rectangular PMUT-on-CMOS is used.

The frequency response of these single-chip PMUTs-on-CMOS systems is not as flat as that of HGL-0085 (a capsule hydrophone). However, their high sensitivities could compensate for this effect once the operation frequency is set and the corresponding sensitivity is established. Furthermore, the possibility of implementing several reading points from different PMUTs on the same chip provides more versatility, giving the option to select which device is most suitable depending on the actuation frequency.

In addition, complementary measurements were carried out from 1 to 20 MHz. Fig. 8 depicts the measured peak-to-peak amplitudes at 9 mm when the OPTEL transducer is excited with 2.4 $V_{pp}$ (HGL-0085 was not included due to its low sensitivity). From the results, the presented PMUTs-on-CMOS hydrophones can transduce the same acoustic pressure into higher voltage amplitudes than the HNC-0200 with smaller areas. Quantifying these enhancements with respect to the commercial hydrophone at the peak frequency (4.8 MHz), the square-shaped PMUT achieves an improvement of 3.3×, the rectangular 2.8×, and the annular 1.6×, respectively.

### B. Minimum Pressure Level

Equation (4) was used to compute the NEP and therefore estimate the minimum pressure level measurable with the hydrophones. To obtain the noise, the acquired rms output voltage signals (for each PMUTs-on-CMOS device) were obtained by taking a time interval without echoes. On the other hand, for the commercial hydrophones, the noise corresponds to the datasheets (see Table I). For verification of the set-up, the rms output voltage signal from the commercial hydrophones has been also acquired obtaining close results to the given by the company. Considering these values and the SR, NEP was computed. Table II summarizes all the results.

According to the illustrated results, the proposed PMUTs-on-CMOS hydrophones will be able to detect acoustic signals with smaller pressure values.

Comparing the data corresponding to the square device and the HGL-0085 hydrophone, the first one provides a 38× factor improvement in the SR (including the amplifier gain), and the ability to detect pressures 67.5 times lower. In addition, note that for rectangular and annular PMUTs-on-CMOS hydrophones, their SR allows for obtaining NEP lower than 200 Pa, which is not possible for the ONDA hydrophones. From these measurements, it can be clearly stated that the PMUTs-on-CMOS presented here outperform commercial hydrophones of equivalent size in terms of receiving loaded sensitivity and NEP.

### C. Maximum Pressure Level

The maximum pressure level for each design was determined based on the saturation that the amplifier shows when high pressures arrive at the PMUTs-on-CMOS surface. This experiment was performed by modifying the peak-to-peak excitation voltages from 250 $mV_{pp}$ to 24 $V_{pp}$ at the OPTEL driving signal (four sinusoidal cycles at 4.8 MHz). This voltage sweep allows us a pressure range from 728 $Pa_{pp}$ to 70.5 $kPa_{pp}$. The temporal response was acquired after 6 $\mu$s which corresponds to a distance of 9 mm between the hydrophone and the transducer from the OPTEL. Fig. 9 top depicts the maximum amplitudes for each device where, as can be seen, the proposed PMUT-on-CMOS hydrophones with minute areas allow us to obtain large amplitudes at the same frequency.

In the same context, the peak-to-peak pressures that can be detected without clamping were determined considering the $P_{1-dB}$ compression points, giving 56, 68, and higher than 80 $kPa_{pp}$ for the square, rectangular, and annular hydrophones-based PMUTs-on-CMOS, respectively. Fig. 9 bottom shows the nonlinearity analysis considering the square PMUT-on-CMOS hydrophone. These levels of pressure are far from the required for some medical applications which could be a limitation of the proposed system in order to characterize different sources. As was discussed in Section II-D, the RX block is the cause of this clamping and not the PMUTs devices, and from the point of view of the proposed design, the source follower output buffer is the main responsible. The topology implemented in this circuit behaves as a voltage level-shifter where to obtain an output resistance of 50 Ω, the dc output voltage is significantly lower than VDD/2. For the used CMOS technology, with dc biasing at 1.5 V, the maximum peak-to-peak pressures with the high SR of our square PMUT-on-CMOS hydrophone could be 789 kPa ( = 1.5 $V_{pp}$/1900 nV/Pa), and this is a limitation that cannot be overcome with this CMOS technology. An alternative to overcome this issue could be implementing a CMOS amplifier with two gains in order to modulate the SR depending on the input pressure. The first gain could be 25 dB for pressure levels lower than 0.8 $MPa_{pp}$, such as has been discussed until now, while the second gain could be adjusted to achieve pressure levels of up to 2 $MPa_{pp}$ which could be obtained considering a loaded SR of 750 nV/Pa, and a dc biasing of 1.5 Vpp.

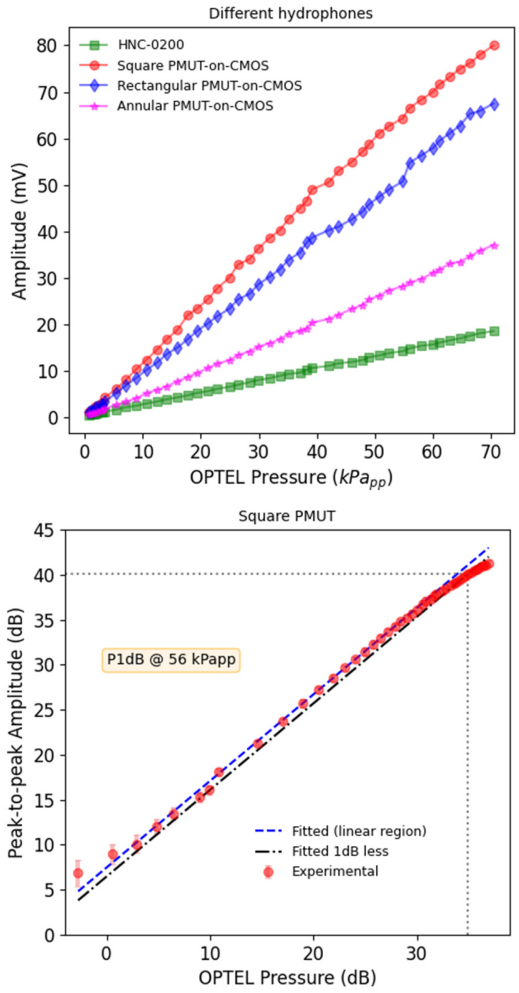


Fig. 9. Experimental points measured by sweeping the peak-to-peak pressure from 728 Papp to 70.5 kPapp. Maximum measured amplitudes considering the HNC-0200 (green squares), square PMUT (red points), rectangular PMUT (blue diamonds), and annular PMUT (magenta stars) (top). Nonlinearity analysis using the square PMUT-on-CMOS (bottom).

TABLE II
SUMMARY OF THE PARAMETERS TO OBTAIN NEP

| Device | Noise(μVrms) | SR (nV/Pa) | NEP (Pa) | Reference |
|---|---|---|---|---|
| Square | 146@22MHz | 1900 | 77 | This work |
| Rectangular | 160@22MHz | 1860 | 86 | |
| Annular | 190@22MHz | 1220 | 156 | |
| HGL-0085 | 260@60MHz | 50 | 5200 | ONDA's hydrophone |
| HNC-0200 | 160@25MHz | 447 | 358 | |

SR: receiving loaded sensitivity (includes amplifier gain).

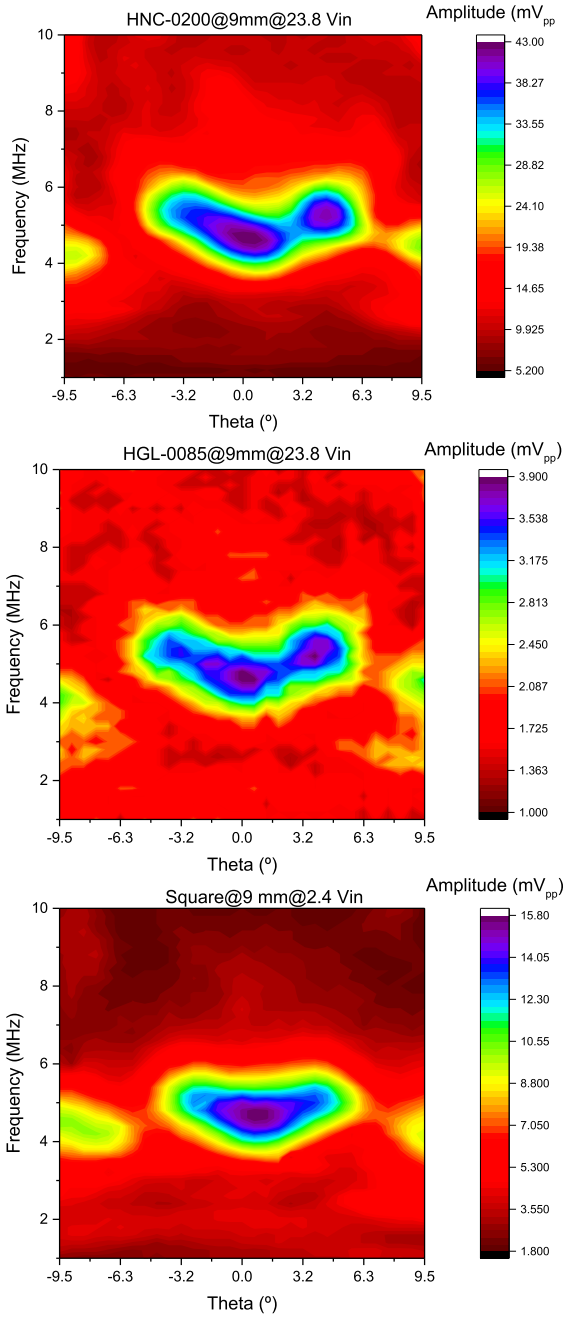


Fig. 10. Hydrophones responses at different lateral positions depending on the actuation frequency. HNC-0200 (top), HGL-0085 (middle), and square PMUT-on CMOS (bottom).

## D. Directional Response

The final aspect to analyze is related to the capability of the presented system not to affect the SR when the angle between the hydrophone and the incident ultrasound wave is different from 0°. For this test, the same commercial transducer from OPTEL was used as a transmitting source and both ONDA's hydrophones and the square PMUT-on-CMOS were used to acquire the acoustic signals. The experiment consists of measuring the acoustic pressure in a frequency range from 1 to 10 MHz displacing each hydrophone 3 mm in the lateral direction and placing it at an axial position of 9 mm. The steps used were 200 kHz in the frequency sweep and 100 $\mu$m in the lateral sweep. The steps used were 200 kHz in the frequency sweep and 100 $\mu$m in the lateral sweep. Fig. 10 shows the 2-D map plots for each device. For the commercial hydrophones HGL-0085 and HNC-0200, the input voltage for the OPTEL transducer was set to 23.8 V, while for the PMUT-on-CMOS hydrophone was 2.4 V. Even with this $\times$10 times lower input voltage, the receiving voltage amplitudes for the presented PMUT-on-CMOS hydrophone were $\times$4 times more than the equivalent in size commercial hydrophone (HGL-0085) while obtaining the same imaging patterns at different directions and operation frequencies.

TABLE III
PMUTs-on-CMOS Hydrophones Characteristics and Comparison With Commercial Hydrophones

| **Parameters** | **PMUTs-on-CMOS** | | | **ONDA** | | **Precision Acoustic** [30] |
|---|---|---|---|---|---|---|
| **Device** | Square | Rectang. | Annular | HGL-0085 | HNC-0200 | NH 0075 |
| **Dimensions** | 80 µm x 80 µm | 60 µm x 40 µm | Out. Diam: 80µm Inn. Diam: 40 µm | Diam. 85 µm | Diam. 200 µm | Diam. 75 µm |
| **Nominal sensitivity, $SR_{EOC}$ (nV/Pa)** | 238 | 447 | 140 | 10[1] | 40[1] | x |
| **Mean loaded sensitivity, *SR* (dB re: 1V/µPa)** | -234 | -234.6 | -238.3 | -266 [1] | -247 [1] | -280 |
| **Mean loaded sensitivity, *SR* (nV/Pa)** | 1900 | 1859 | 1220 | 50 | 447 | 10 |
| **NEP (Pa)** | 77 | 86 | 156 | 5200[2] | 358[2] | 1897[2] |

[1] Extracted from the provided calibration by the company.
[2] Computed value considering output-referred voltage noise spectral density in the amplifier bandwidth and the mean sensitivity.

## V. Conclusion

In this article, a novel hydrophone based on minute PMUTs-on-CMOS was discussed. The presented single-chip hydrophone (with an area of 1.9 × 1.5 mm) provides three designs (square, rectangular, and annular PMUTs) integrated monolithically with a CMOS-LNA amplifier. A preliminary prototype was characterized in water and compared with two commercial hydrophones from ONDA, HGL-0085, and HNC-0200, where the main results show competitive values. Table III summarizes the main characteristics of the PMUTs-on-CMOS LNA working as hydrophones and a comparison with some commercial. In this context, it is important to highlight the high sensitivities achieved, which are around −236 dB (mean value considering the three PMUTs-on-CMOS) instead of −266 dB for a hydrophone of almost the same dimensions (HGL-0085 + Preamplifier), or −247 dB for a larger hydrophone (HNC-0200) + Preamplifier). Another benefit is regarding the NEP, where pressure levels lower than 150 Pa could be detected by the PMUTs-on-CMOS systems.

This new approach of hydrophone design based on PMUTs integrated monolithically with the CMOS circuitry opens a way to develop on a single chip several independent reading points which could open new strategies for acoustic field detection, with a high sensitivity, a low noise, and the capability to place them close to the transmitting source.

## Acknowledgment

The authors would like to specifically acknowledge Eloi Marigó Ferrer and all the other members of SilTerra's MEMS and SENSORS technology development team for supporting the fabrication of the PMUT-on-CMOS wafers.

## References

[1] A. Hurrell and P. Beard, "Piezoelectric and fibre-optic hydrophones," in *Ultrasonic Transducers*. Baltimore, MD, USA: Wood, 2012, pp. 619–676.

[2] T. Şen, O. Tüfekçioğlu, and Y. Koza, "Mechanical index," *Anatol. J. Cardiol.*, vol. 15, no. 4, pp. 334–336, 2015.

[3] G. R. Harris et al., "Hydrophone measurements for biomedical ultrasound applications: A review," *IEEE Trans. Ultrason., Ferroelectr., Freq. Control*, vol. 70, no. 2, pp. 85–100, Feb. 2023.

[4] J. M. Rothberg et al., "Ultrasound-on-chip platform for medical imaging, analysis, and collective intelligence," *Proc. Nat. Acad. Sci. USA*, vol. 118, no. 27, pp. 1–18, Jul. 2021.

[5] G. Li et al., "Noninvasive ultrasonic neuromodulation in freely moving mice," *IEEE Trans. Biomed. Eng.*, vol. 66, no. 1, pp. 217–224, Jan. 2019.

[6] C. Yu et al., "A conformable ultrasound patch for cavitation-enhanced transdermal cosmeceutical delivery," *Adv. Mater.*, vol. 35, no. 23, Jun. 2023, Art. no. 2300066.

[7] H. Saheban and Z. Kordrostami, "Hydrophones, fundamental features, design considerations, and various structures: A review," *Sens. Actuators A, Phys.*, vol. 329, Oct. 2021, Art. no. 112790.

[8] (2020). *ONDA Corporation*. Accessed: Oct. 5, 2023. [Online]. Available: https://www.ondacorp.com/

[9] (2023). *Precision Acoustics*. Accessed: Oct. 5, 2023. [Online]. Available: https://www.acoustics.co.uk/

[10] O. Ivanytskyy, G. Pang, A. Burhoe, M. Moszczynski, and N. C. Chaggares, "Membrane hydrophone for high frequency ultrasound and method of manufacture," U.S. Patent 10 451 476 B2, Oct. 22, 2023.

[11] N. Chris Chaggares, O. Ivanytskyy, and G. Pang, "Design of a 30 um aperture membrane hydrophone for the measurement and characterization of high frequency ultrasound," in *Proc. IEEE Int. Ultrason. Symp. (IUS)*, Sep. 2016, pp. 1–6.

[12] J. Janjic et al., "A 2-D ultrasound transducer with front-end ASIC and low cable count for 3-D forward-looking intravascular imaging: Performance and characterization," *IEEE Trans. Ultrason., Ferroelectr., Freq. Control*, vol. 65, no. 10, pp. 1832–1844, Oct. 2018.

[13] P. Cristman et al., "A 2D CMUT hydrophone array: Characterization results," in *Proc. IEEE Int. Ultrason. Symp.*, Sep. 2009, pp. 992–995.

[14] L. Jia, L. Shi, C. Liu, Y. Yao, C. Sun, and G. Wu, "Design and characterization of an aluminum nitride-based MEMS hydrophone with biologically honeycomb architecture," *IEEE Trans. Electron Devices*, vol. 68, no. 9, pp. 4656–4663, Sep. 2021.

[15] T. Yang et al., "Design and implementation of 6 × 6 array piezoelectric AlN hydrophone with high sensitivity," *IEEE Sensors J.*, vol. 21, no. 23, pp. 26615–26623, Dec. 2021.

[16] L. Jia, L. Shi, Z. Lu, C. Sun, and G. Wu, "A high-performance 9.5% scandium-doped aluminum nitride piezoelectric MEMS hydrophone with honeycomb structure," *IEEE Electron Device Lett.*, vol. 42, no. 12, pp. 1845–1848, Dec. 2021.

[17] Onda Corp. (2023). *Hydrophone Handbook*. Accessed: Oct. 10, 2023. [Online]. Available: http://ondacorp.com/Handbook/mobile/index.html
[18] J. Lim, C. Tekes, E. F. Arkan, A. Rezvanitabar, F. L. Degertekin, and M. Ghovanloo, "Highly integrated guidewire ultrasound imaging system-on-a-chip," *IEEE J. Solid-State Circuits*, vol. 55, no. 5, pp. 1310–1323, May 2020.
[19] R. A. Smith, "Are hydrophones of diameter 0. 5 mm small enough to characterise diagnostic ultrasound equipment?" *Phys. Med. Biol.*, vol. 34, pp. 1607–1953, Oct. 1989.
[20] K. A. Wear and A. Shah, "Nominal versus actual spatial resolution: Comparison of directivity and frequency-dependent effective sensitive element size for membrane, needle, capsule, and fiber-optic hydrophones," *IEEE Trans. Ultrason., Ferroelectr., Freq. Control*, vol. 70, no. 2, pp. 112–119, Feb. 2023.
[21] S. Umchid, "Spatial averaging correction for ultrasound hydrophone calibrations," *Int. J. Appl. Biomed. Eng.*, vol. 9, no. 1, pp. 33–38, 2016.
[22] *Ultrasonics—Hydrophones—Part 1: Measurement and Characterization of Medical Ultrasonic Fields Up To 40 MHz*, Standard IEC 62127-1-2007, 2007, p. 170.
[23] D. T. Blackstock, *Fundamentals of Physical Acoustics*. Hoboken, NJ, USA: Wiley, 2000.
[24] E. Ledesma, I. Zamora, J. Yanez, A. Uranga, and N. Barniol, "Single-cell system using monolithic PMUTs-on-CMOS to monitor fluid hydrodynamic properties," *Microsystems Nanoengineering*, vol. 8, no. 1, p. 76, Jul. 2022.
[25] I. Zamora, E. Ledesma, A. Uranga, and N. Barniol, "Phased array based on AlScN piezoelectric micromachined ultrasound transducers monolithically integrated on CMOS," *IEEE Electron Device Lett.*, vol. 43, no. 7, pp. 1113–1116, Jul. 2022.
[26] C. Seok, O. J. Adelegan, A. Ö. Biliroglu, F. Y. Yamaner, and Ö. Oralkan, "A wearable ultrasonic neurostimulator—Part II: A 2D CMUT phased array system with a flip-chip bonded ASIC," *IEEE Trans. Biomed. Circuits Syst.*, vol. 15, no. 4, pp. 705–718, Aug. 2021.
[27] X. Jiang et al., "Monolithic ultrasound fingerprint sensor," *Microsystems Nanoengineering*, vol. 3, no. 1, p. 17059, Nov. 2017.
[28] Optel. *OPTEL Ultrasonic Technology*. Accessed: May, 20, 2022. [Online]. Available: https://optel.eu/index.html
[29] I. Zamora, E. Ledesma, A. Uranga, and N. Barniol, "Monolithic single PMUT-on-CMOS ultrasound system with +17 dB SNR for imaging applications," *IEEE Access*, vol. 8, pp. 142785–142794, 2020.
[30] Precis. Acoust. Ltd. *0.075 Mm Needle Hydrophone (NH0075)*. Accessed: Oct. 23, 2023. [Online]. Available: https://www.acoustics.co.uk/product/75-micron-needle-hydrophone/

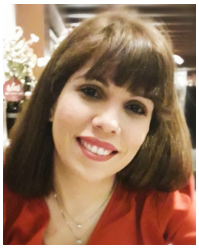

**Eyglis Ledesma** received the B.Sc. degree in telecommunication and electronic engineering from the Havana University of Technology José Antonio Echevarria, La Habana, Cuba, in 2014, and the Ph.D. degree in electronic and telecommunications engineering from Universitat Autònoma de Barcelona, Barcelona, Spain, in 2022.

She is a Postdoctoral Researcher at Universitat Autònoma de Barcelona. Her research interests include piezoelectric micro-electro-mechanical-system (MEMS) devices for ultrasonic sensor applications.

**Arantxa Uranga** received the B.Sc. degree in physics and the B.Sc. degree electronics engineering from Valladolid University, Valladolid, Spain, in 1994 and 1996, respectively, and the Ph.D. degree in electronics engineering from the Universitat Autònoma de Barcelona, Barcelona, Spain, in 2001.

Since 1996, she has been with the Department of Electronics Engineering, Universitat Autònoma de Barcelona, where she is currently an Associate Professor. Her research interests include the design of complementary metal-oxide-semiconductor (CMOS) circuits for radio frequency (RF) processing and sensor applications, focusing on micro-electro-mechanical-system (MEMS)/nano-electromechanical-systems (NEMS) devices.

**Núria Barniol** (Member, IEEE) received the Ph.D. degree in physics from the Universitat Autònoma de Barcelona (UAB), Barcelona, Spain, in 1992.

She is currently a Full Professor at the Department of Electronics Engineering, UAB. She has been working for the last 20 years in the field of micro-electro-mechanical-system (MEMS) resonators and their integration within complementary metal-oxide-semiconductor (CMOS) technologies focused on the reduction of dimensions toward nanoelectromechanical devices with optimized CMOS conditioning circuitry. She has coauthored more than 100 research articles and 200 peer-reviewed conferences. Her research interests include the study of novel piezoelectrical micro/nanometric ultrasonic transducers, their integration with CMOS toward efficient biometrics systems, and the exploitation of nonlinear nano-electromechanical-systems (NEMS) resonators.

Dr. Barniol was a recipient of the Award of the Universitat Autónoma de Barcelona, for Research Excellence in the area of technology, in 2009. She was on the Program Committee of several conferences, including IEEE International Electron Devices Meeting (IEEE-IEDM), IEEE International Conference on Micro Electro Mechanical Systems (IEEE-MEMS), Microand Nano Engineering Conference (MNE), Transducers, and Eurosensors.